Langmuir

Article

pubs.acs.org/Langmuir

In Situ Fabricated Polymer–Silver Nanocomposite Thin Film as an Inexpensive and Efficient Substrate for Surface-Enhanced Raman Scattering

E. Hariprasad and T. P. Radhakrishnan*

School of Chemistry, University of Hyderabad, Hyderabad 500 046, India

Supporting Information

ABSTRACT: The utility of polymer–metal nanocomposite thin films with *in situ* generated silver nanoparticles as substrates for surface-enhanced Raman scattering (SERS) is demonstrated. Thin films of poly(vinyl alcohol) and poly(vinyl butyral-*co*-vinyl alcohol-*co*-vinyl acetate) containing Ag nanoparticles generated *in situ* through thermal annealing and photoirradiation, respectively (Ag–PVA and Ag–PVVV), are investigated as potential SERS substrates using 4-aminothiophenol and rhodamine 6G as probe molecules. The fabrication protocols are extremely simple and the materials inexpensive. The Ag–PVA substrate is found to produce Raman spectral enhancement factors of ~10^6, whereas Ag–PVVV, a novel nanocomposite thin film developed in the present study, provides enhancement factors of ~10^7. A unique advantage of these nanocomposite films is demonstrated by fabricating them by the *in situ* process as a thin coating inside glass capillaries and using these disposable SERS substrates for the sensitive detection of the probe molecules. The thin film substrates prepared on glass plates and capillaries facilitate convenient sample preparation for recording the Raman spectra and provide strongly enhanced spectra with high reproducibility, allowing picomols of the analytes to be detected. These aspects combined with the ease of fabrication and low cost of these *in situ* fabricated nanocomposite thin films make them highly attractive SERS substrates.

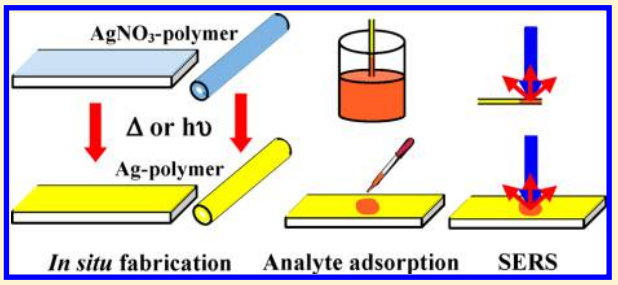

INTRODUCTION

The enhanced Raman scattering of molecules adsorbed on rough metal surfaces and especially metal nanoparticles and nanostructures (surface-enhanced Raman scattering, SERS) serves as a highly sensitive detection tool.[1−3] Nanostructures of noble metals such as silver and gold are preferred, as visible light can be used to excite their localized surface plasmon resonance (LSPR) and exploit the resulting local electromagnetic field. A wide range of substrates have been developed based on these nanoparticles and nanostructures for adsorbing molecules and observing their SERS.[4] The simplest structure would be a monolayer of the nanoparticles on substrates like silicon wafer[5] or polymer thin film.[6,7] Interesting variations on this approach include the use of temperature-sensitive polymer membranes[8] and conducting polymer fibers.[9] Other substrates used for assembling metal nanoparticles and nanostructures include graphene[10] and graphene oxide,[11] glass capillary,[12] silicon nanopillar,[13] core–shell microsphere,[14] porous alumina membrane,[15] and unconventional choices like filter paper,[16] inkjet printed cellulose paper,[17] and aluminum foil.[18] Nanogap[19,20] and nanodome[21] arrays, nanodroplets on nanowall networks,[22] plasmonic lenses,[23] and metastable nanoparticle film[24] have also been developed as efficient SERS substrates.

Important considerations for the development of a SERS substrate are the cost of materials, ease of fabrication, durability, facility of use, and of course sensitivity and reproducibility of the Raman spectral measurements. Polymer–metal nanocomposite thin films offer one of the simplest designs that address the wide range of requirements. Poly(vinyl alcohol) (PVA) is a particularly convenient choice for the polymer. A SERS substrate has been developed using a nanocomposite prepared from Ag nanoparticles formed in solution using PVA and poly(γ-glutamic acid) as reductant and stabilizer.[25] PVA film containing silver generated using ferrous sulfate as the reducing agent has been shown to produce SERS response;[26] however, this study did not provide any details of the silver nanoparticles or the spectral enhancement factor. Another substrate design involved electrospun PVA nanofibers with aligned silver nanoparticles.[27] We have developed earlier a simple and facile protocol for the *in situ* generation of silver nanoparticles inside PVA thin films,[28,29] the PVA acting simultaneously as the reducing agent as well as the matrix for stabilization of the generated nanoparticles. An aqueous solution containing $AgNO_3$ and PVA is spin-coated on a suitable substrate and subjected to thermal annealing leading to the generation of a homogeneous and monodisperse distribution of silver nanoparticles within the film. The method is environmentally benign, allows convenient monitoring of the nanoparticle formation,[30,31] and produces free-standing thin films that can be directly imaged in a transmission electron

Received: July 11, 2013
Revised: September 19, 2013
Published: October 9, 2013

   dx.doi.org/10.1021/la402594j | *Langmuir* 2013, 29, 13050–13057

microscope. In earlier studies, we have demonstrated the application of these nanocomposite thin films as optical limiter,[28,32] bactericide,[33] catalyst,[34,35] and chemical sensor.[36]

We have now explored the utility of *in situ* synthesized polymer−metal nanocomposite thin films as easily fabricated and inexpensive SERS substrates. Ag−PVA thin film prepared using our protocol described above is found to be a durable SERS substrate showing enhancement factors (EF) of $\sim 10^6$ with good reproducibility. In order to explore the possibility of achieving higher EF in similar substrates, we have investigated several variants of PVA, as these can influence considerably the surface morphology of the thin films as well as the size and shape of the silver nanoparticles generated within. Thin film of poly(vinyl butyral-*co*-vinyl alcohol-*co*-vinyl acetate) (PVVV) with the silver nanoparticles generated *in situ* by photoirradiation is identified as an efficient SERS substrates with EF of $\sim 10^7$. We present the details of the fabrication and characterization of these substrates followed by their deployment as SERS substrates. We also demonstrate the fabrication of a glass capillary with the Ag−polymer thin film coated on the inner walls that serves as a cheap and disposable SERS substrate.

EXPERIMENTAL SECTION

Fabrication of Ag−PVA Substrate. 18.9 mg of silver nitrate ($AgNO_3$; Aldrich, purity = 99.9+%) dissolved in 0.3 mL of water was mixed with 0.6 mL of a solution of PVA (Aldrich, average molecular weight = 85−146 kDa, % hydrolysis = 99+%) in water (1.0 g of PVA in 20 mL of water). The Ag/PVA weight ratio (x) is 0.4; solutions with other ratios were also prepared by altering the amount of $AgNO_3$. The solution mixture was stirred for 10 min at 25 °C. Millipore Milli-Q purified water was used in all operations. Silicon wafers were cleaned in soap solution and water followed by sonication with isopropyl alcohol for 10 min and dried under nitrogen flow. The $AgNO_3$−PVA solution was spin-coated on the wafer (typically 2.5 × 1.2 cm^2) using a Laurell Technologies Corporation Model WS-650HZ-23NPP/LITE single wafer spin processor operated at 500 rpm for 10 s followed by 10 000 rpm for 10 s. The film was heated in a hot air oven at 130 °C for 3 h to generate *in situ* the silver nanoparticles within the film.

Fabrication of Ag−PVVV Substrate. The approach is similar to that used for Ag-PVA but with some significant changes. 40.0 mg of PVVV (Aldrich; average molecular weight = 70−100 kDa; wt % vinyl butyral 80, vinyl alcohol 18−20, vinyl acetate 0−1.5) and the required amount of $AgNO_3$ (for example, 24.0 mg gives an Ag/PVVV weight ratio x = 0.4) were added to 1.2 mL of ethanol and stirred for 10 min at 25 °C. The $AgNO_3$−PVVV solution was spin-coated on Si wafer at 8000 rpm for 10 s. The film was either heated in a hot air oven at 130 °C or UV-irradiated (λ = 254 nm) in a photoreactor (Scientific Aids & Instruments Corporation model MLR-8) for 3 h. The latter procedure was found to be a more efficient method to produce *in situ* silver nanoparticles inside the PVVV film.

Characterization of the Nanocomposite Thin Films. The thickness of the films was measured using an Ambios Technology XP-1 profilometer. LSPR extinction spectra of films coated on glass/quartz were recorded on a Varian Model Cary 100 UV−vis spectrometer in transmission mode; spectra of films coated on Si wafer were recorded in diffuse reflectance mode using the DRA-CA-30I accessory and converted to absorption spectra using the Kubelka−Munk function. Atomic force microscope (AFM) images of the films on Si wafer were recorded using an NT-MDT model Solver pro-M AFM in semicontact mode using a cantilever with a force constant of 12 N/m; roughness was analyzed using the software provided by the manufacturer. Scanning electron microscopy (SEM) was carried out on a Philips XL 30 ESEM, HITACHI_S3400N SEM, or Carl Zeiss model Ultra 55 (FESEM) microscope. Transmission electron microscope (TEM) images were recorded on an FEI model TECNAI G^2 S-Twin TEM at an accelerating voltage of 200 kV. Free-standing film samples of Ag-PVA for the imaging were prepared as follows. A few drops of a solution of 1 g of polystyrene (PS, average molecular weight = 280 kDa) in 8 mL of toluene was spin-coated on a glass substrate at 1000 rpm for 10 s, followed by drying in a hot air oven at 85−90 °C for 20 min. The $AgNO_3$−PVA solution was coated on top of the PS layer by spinning at 500 rpm for 10 s followed by 10 000 rpm for 10 s and subsequently subjected to thermal treatment. The film was then cut, peeled off the glass, and placed on a 200 mesh TEM copper grid and dipped in toluene, whereupon the PS layer dissolved out. As PVVV is soluble in toluene this method cannot be used; samples were prepared by coating the $AgNO_3$−PVVV solution directly on carbon-coated copper grids and subjecting them to UV irradiation as mentioned earlier.

SERS Experiments. 4-Aminothiophenol (4-ATP; Aldrich, purity 97%) and Rhodamine 6G (R6G; Loba Chemie) recrystallized from methanol solutions were used as the probe molecules. Choice of these standard probe molecules was prompted by the fact that the former is capable of engaging in strong chemical interactions with the silver nanoparticles through the thiol group and the latter is not. Typically, 1−100 μM solutions of the probe molecules were prepared in HPLC grade methanol. 10 μL of the solution was spread homogeneously on the substrate and allowed to dry for 30 min. Raman spectra were recorded using a WITec model Alpha 300 R Raman microscope (with AFM), with 0.5 s integration time and 10 accumulations, through a 50× aperture (NA = 0.8). Excitation wavelengths of 633 and 488 nm were used respectively for 4-ATP and R6G; wavelengths away from and close to the LSPR extinction peak of the silver nanoparticles were chosen so as to test the efficiency of our SERS substrate without and with strong contribution from the local electromagnetic field effects. The laser intensity was maintained constant in all measurements, and a 25 μm detecting fiber was used to collect the Raman spectra. Special care taken to use sufficiently low laser power in order to avoid photochemical processes, is described at the appropriate point in the Results and Discussion section. The Raman spectrum corresponding to the bulk material was collected using a microcrystal placed on a silicon wafer; identity and purity of the crystal were confirmed by X-ray diffraction analysis.[37]

The SERS EF was estimated using the approach discussed in earlier studies[38,39] adapted for the current experimental protocol. EF is given by the general expression

$$\mathrm{EF} = \frac{I_{\mathrm{SERS}}}{I_{\mathrm{Bulk}}}\frac{N_{\mathrm{bulk}}}{N_{\mathrm{SERS}}}$$

where I is the intensity of a Raman signal and N is the number of molecules within the laser spot (giving rise to the signal), in the focal volume of the beam in a single crystal of the analyte (Bulk) and the solution adsorbed on the SERS substrate (SERS). It should be stressed that N_{SERS} includes all the probe molecules in the focal volume and not just a monolayer on the nanoparticles; hence, the EF determined is the lower bound of this value. For the current experiment, the ratio of the number of molecules in the two cases can be shown to be[37]

$$\frac{N_{\mathrm{bulk}}}{N_{\mathrm{SERS}}} = \frac{2344\lambda}{NA^2}A\frac{\rho}{w}$$

where λ is the wavelength of the laser light (nm), NA the numerical aperture, A the total area over which the analyte solution is spread on the SERS substrate (cm^2), ρ the density of the analyte crystal (g cm^{-3}), and w the weight of the analyte in the solution spread on the film (ng).

RESULTS AND DISCUSSION

Initial experiments were carried out using Ag−PVA thin films fabricated using the *in situ* approach and thermal annealing for the formation of the silver nanoparticles. A series of experiments were used to determine the optimal concentration of silver nanoparticles (by varying the Ag/PVA weight ratio, x) and the thin film thickness (by varying the solution viscosity

dx.doi.org/10.1021/la402594j | *Langmuir* 2013, 29, 13050−13057

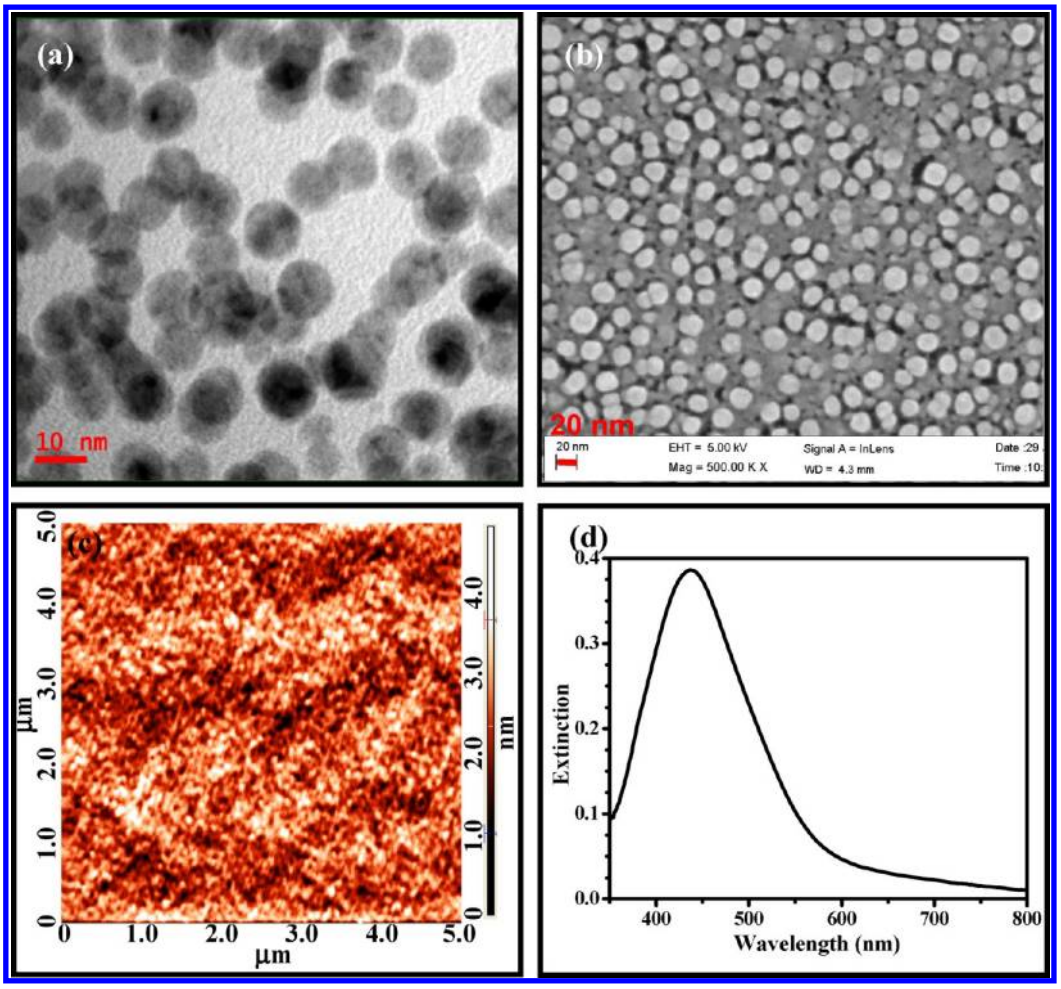

Figure 1. (a) TEM image (scale bar = 10 nm), (b) FESEM image (scale bar = 20 nm), (c) AFM image (5 μm × 5 μm), and (d) LSPR extinction spectrum of Ag−PVA thin film (x = 0.4).

and spin-coating conditions) that will lead to the maximum sensitivity of detection in terms of the EF. The SERS efficiency increased significantly when x was increased from 0.2 to 0.4, but less prominently at still higher loadings of silver;[37] this point is discussed in detail in the context of Ag−PVVV below. Within the limits of the parameters we tested, the best substrate was thus obtained using x = 0.4 and a film thickness of 110 ± 8 nm (obtained with spin-coating speeds of 10 krpm). TEM image of the free-standing film (Figure 1a) shows a homogeneous distribution of nearly spherical Ag nanoparticles, ∼9−12 nm in diameter. FESEM image of the film directly coated on a Si wafer showed Ag nanoparticles ∼15−20 nm in diameter (Figure 1b); change in the size distribution is likely to be due to the difference in the substrate. The AFM image of the film on Si wafer is shown in Figure 1c; the film is extremely smooth with an average surface roughness of 0.7 ± 0.1 nm. The LSPR extinction spectrum of the film shows a λ_{max} ∼ 437 nm (Figure 1d). Experiments with solutions containing typically 30−100 pmol of 4-ATP and R6G gave Raman spectra with EF in the range of 10^5−10^6.[37] Since the Ag−PVA films contain Ag nanoparticles with dimensions that are relatively small compared to the film thickness and the film surface is very smooth, it appears that the access of the nanoparticle to the analyte molecules is limited. Therefore, we have sought to fabricate thin films containing relatively larger Ag nanoparticles and having a higher surface roughness. As PVA and the thermal annealing protocol were not ideally suited for this, we have explored related polymers and modifications in the *in situ* fabrication method to prepare novel polymer−silver nanocomposite thin films.

Based on the trial experiments with different polymers containing the hydroxy functionality that is essential to reduce the silver ions to silver atoms in the formation of the nanoparticles, PVVV was found to be the best choice. In the case of PVVV, photoirradiation rather than thermal annealing turns out to be a more efficient route to generate *in situ* the silver nanoparticles inside the solid polymer film. The thin film formed under the optimized fabrication conditions was typically ∼270 ± 60 nm thick. TEM images of the films with x = 0.4 show Ag nanoparticles with two different size distributions: 2−5 nm and 25−100 nm (Figure 2a). The FESEM image is broadly consistent with this observation, showing the larger particles clearly (Figure 2b). The particle morphologies range from nearly spherical to plate-like. AFM images show that the film surface has a roughness of the order of 8.0 ± 2.3 nm (Figure 2c), considerably higher than that of the Ag−PVA film. The LSPR extinction spectrum with λ_{max} ∼ 450 nm and a shoulder at ∼575 nm is consistent with the formation of Ag nanoparticles with different sizes and shapes including relatively large and nonspherical ones (Figure 2d).

The efficiency of the Ag−PVVV film as a SERS substrate was tested using 4-ATP and R6G analyte molecules. The Raman

dx.doi.org/10.1021/la402594j | *Langmuir* 2013, 29, 13050−13057

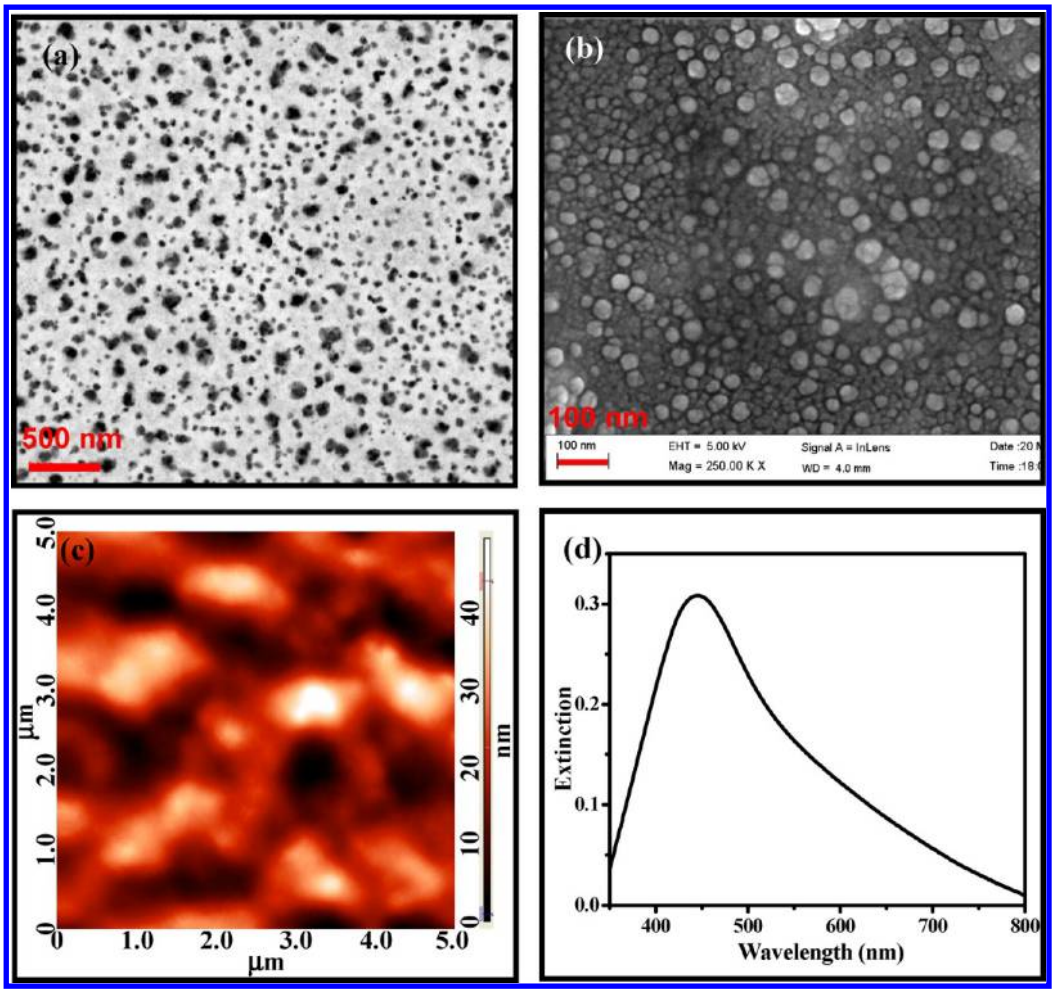

Figure 2. (a) TEM image (scale bar = 500 nm), (b) FESEM image (scale bar = 100 nm), (c) AFM image (5 μm × 5 μm), and (d) LSPR extinction spectrum of Ag–PVVV thin film (x = 0.4).

spectra recorded for the bulk crystalline samples of the analytes and for the solutions containing ~30 pmol of the analyte spread uniformly on the substrate thin film are shown in Figures 3 and 4 (Ag–PVVV film prepared by thermal annealing produced very little SERS effect).[37] Homogeneous spreading of the solution was confirmed by recording the spectra at different points on the film. The strong electronic absorption in the case of R6G also helped to confirm the homogeneous distribution of

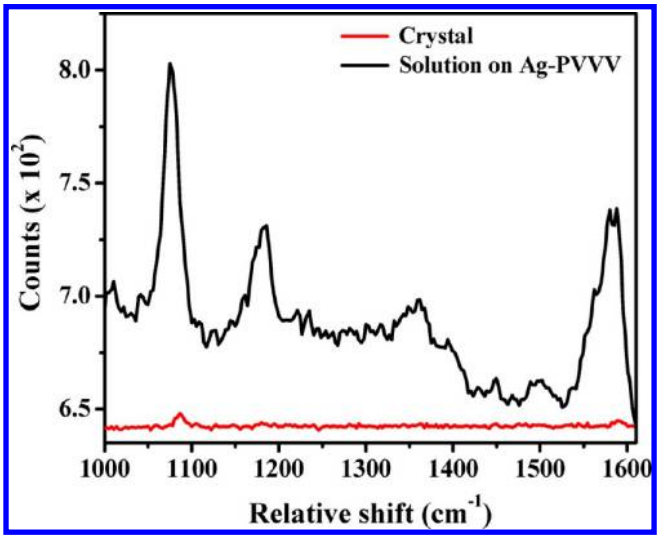

Figure 3. Raman spectra of 4-ATP crystal and 4-ATP solution adsorbed on Ag–PVVV (x = 0.4) thin film substrate.

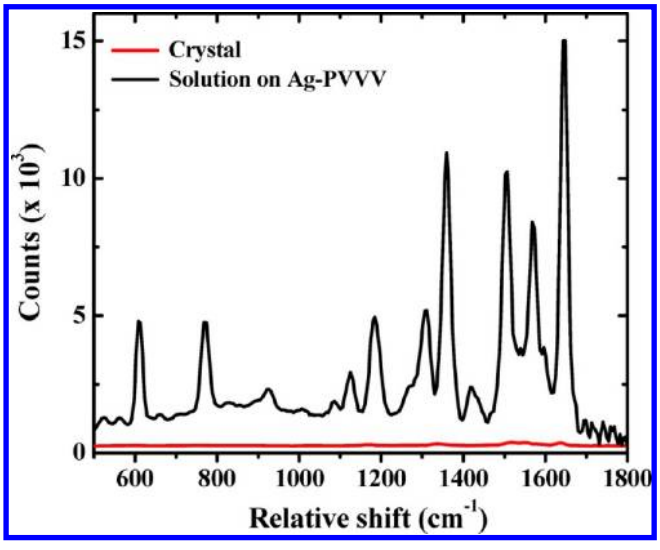

Figure 4. Raman spectra of R6G crystal and R6G solution adsorbed on Ag–PVVV (x = 0.4) thin film substrate (corrected for fluorescence background).

dx.doi.org/10.1021/la402594j | Langmuir 2013, 29, 13050–13057

the analyte molecules over the substrate film.[37] In the case of 4-ATP, several earlier studies have shown that the enhanced signals can arise from 4,4′-dimercaptoazobenzene photogenerated during the Raman experiment.[40,41] We have recorded the spectra using different laser powers; with the present substrates it was found that the peaks at ∼1140, ∼1390, and 1440 cm^{-1}, attributed to the dimer,[41] do not appear up to a power of ∼100 kW/cm^2. Therefore, we have carried out all the SERS studies with 4-ATP using a laser power of 50.0 kW/cm^2, precluding the possibility of 4-ATP undergoing a photochemical change (compare Figure 3 with those recorded at higher laser powers[41]). The spectra of 4-ATP on the nanocomposite thin film show the small, but characteristic, red-shifts of the peaks (1075, 1583 cm^{-1}) relative to those of the bulk crystals (1086, 1590 cm^{-1}). This is commonly attributed to the impact of chemical interaction between the silver nanoparticle surface and the adsorbed thio compound.[42]

The EF estimated for the 4-ATP and R6G molecules on the Ag−PVVV film with different spectral peaks as markers are collected in Tables 1 and 2 (calculation of the EF is described in the Experimental Section). In both cases (4-ATP and R6G) the EF's are found to be ∼10^7. The values estimated for the different vibrational transitions fall within a narrow range. Similar enhancement observed in the case of the two different probe molecules indicates that the present observations are indeed due to SERS; possible impact of photochemical processes in the case of 4-ATP can be ruled out. Repeated experiments on Ag−PVVV substrates fabricated in several different batches showed a high level of reproducibility of the surface-enhanced Raman spectra and the EF values.[37] The limits of detection (defined as $3\sigma_{blank}/m$ where σ_{blank} is the standard deviation for blank measurements and m is the slope for the calibration plot)[37,43,44] for 4-ATP and R6G on Ag−PVVV are found to be respectively 86 and 55 pmol. These values are based on the total solution spread on the substrate; the values would be much smaller if only those in the focal volume are considered. We believe that both electromagnetic field and chemical interactions play a role in the SERS of 4-ATP, whereas it is likely to be mostly the former effect in the case of R6G; it may also be noted that the electromagnetic field contribution may not be very high when the excitation wavelength is away from the LSPR peak. The EF observed with these easily fabricated, cheap, and durable SERS substrates is quite high. This factor coupled with the good reproducibility of the spectra demonstrates the high utility of the *in situ* synthesized polymer−metal nanocomposite thin films for analytical applications. The Ag−PVVV films can be stored under normal atmosphere and ambient conditions for several months without any significant loss of the original LSPR characteristics and SERS efficiency.

Table 1. Intensity of the Raman Spectral Peaks (I) of a Crystal of 4-ATP and a Solution of 4-ATP (Containing ∼90 pmol) on Ag−PVVV (x = 0.4) as the Substrate (Figure 3) along with the Enhancement Factor (EF) in Each Case

bulk		SERS		
peak (cm^{-1})	I	peak (cm^{-1})	I	EF (10^7)
1086	5.6	1075	115	1.3
1590	2.8	1583	88	2.0

Table 2. Intensity of the Raman Spectral Peaks of a Crystal of R6G (I_{BULK}) and a Solution of R6G (Containing ∼30 pmol) on Ag−PVVV (x = 0.4) as the Substrate (I_{SERS}) (Figure 4) along with the Enhancement Factor (EF) in Each Case

peak (cm^{-1})	I_{BULK}	I_{SERS}	EF (10^7)
608	17.4	3487.6	9.1
768	16.0	2931.4	8.3
1194	29.0	2433.9	3.8
1364	28.0	7939.0	12.9
1573	31.4	3248.5	4.7
1648	78.2	10779.7	6.3

Dependence of the EF on x is similar to that mentioned in the case of Ag-PVA; the increase in EF is significant on increasing x from 0.2 to 0.4, but less prominent on further increase. An insight into this can be gained from the LSPR extinction spectra of these nanocomposite thin films (Figure 5).

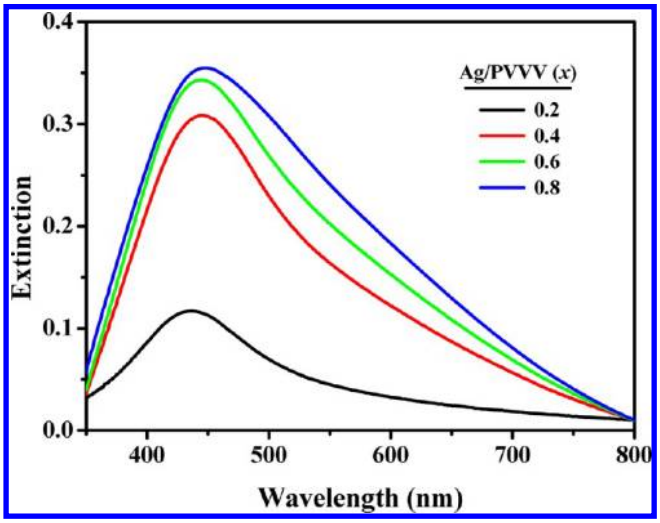

Figure 5. LSPR extinction spectra of Ag−PVVV thin films with different Ag/PVVV weight ratios.

When x increases from 0.2 to 0.4, the prominent change is the enhancement of the extinction, suggesting an increase in the population of nanoparticles; a small broadening of the spectrum is also observed. When x increases further, the extinction increases very little, but the broadening becomes more conspicuous, indicating nanoparticle aggregation. While the increase in the density of nanoparticles promotes the SERS enhancement due to the increased surface area available, their aggregation affects it adversely.

Use of oriented silver nanowires deposited on the inner walls of a capillary as SERS substrate has been reported.[12] However, this fabrication involved a multistep procedure for the synthesis of the nanowires followed by a flow protocol for assembling them inside the capillary, the latter step requiring relatively large amounts of silver nanowires. We have probed a unique advantage of the *in situ* fabricated nanocomposite thin film as SERS substrate by forming it on the inner walls of a glass capillary. Mixtures of the solutions of $AgNO_3$ and PVA/PVVV were prepared, and a very small volume (typically 0.5−1.0 μL) was sucked into a glass capillary (i.d. ∼ 600 μm). After removing traces of the solution that may be sticking on the outside wall, the capillary was heated inside a hot air oven at 130 °C (Ag-PVA) or UV irradiated (Ag−PVVV) for about 3 h. The solution dries, and the *in situ* reduction of the silver ions to

dx.doi.org/10.1021/la402594j | *Langmuir* 2013, 29, 13050−13057

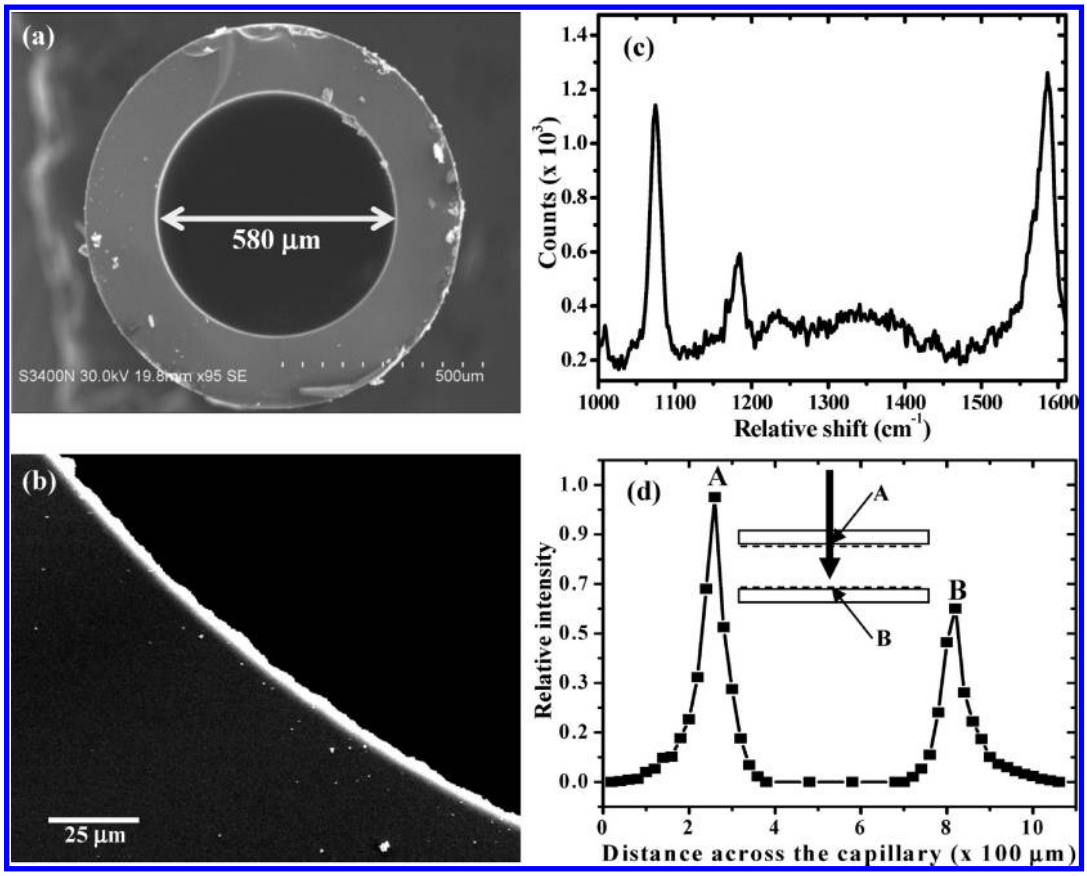

Figure 6. (a) SEM image of the cross section of the capillary with an inner lining of Ag–PVA thin film, (b) magnified view of the inner wall showing the film coating, (c) a typical SERS spectrum of 4-ATP adsorbed on the Ag-PVA film coating inside the capillary, and (d) plot of the signal intensity of the 1075 cm^{-1} peak of 4-ATP as a function of the point of focus across the diameter of the capillary (the schematic diagram shows the orientation of the capillary, the laser beam, and the points where the beam meets the Ag–PVA film coating containing 4-ATP).

Ag nanoparticles imparts a deep yellow color to the film coated on the inner wall of the capillary. The SEM images in Figures 6a,b show the cross section of the glass capillary and the thin film coating; the coating is estimated to be ~4 μm thick. The presence of the silver nanoparticles is confirmed by recording the EDX spectrum of the coated region.[37]

In order to test the analyte, ~0.5 μL of an 8.8 μM solution of 4-ATP was sucked into the capillary and allowed to get absorbed on the polymer coating lining the capillary. After drying, the capillary was placed directly in the Raman microscope so that the laser beam can be directed across the diameter. The beam was focused at different levels across the capillary, and the spectra were recorded (10× objective (NA = 0.25) was used). When the focal spot is in the region of the polymer film, clear spectra could be recorded; a typical spectrum is shown in Figure 6c. It is important to note that the molecular content sucked into the capillary is as low as 5 pmol and that the exact amount of molecules that come under the laser spot will be even smaller. The intensity of the 1075 cm^{-1} peak of 4-ATP is plotted against the focal position across the diameter of the capillary (Figure 6d). The two peaks separated by ~560 μm correspond to the beam focusing on the coatings across the inner diameter at positions A and B. Peak B is relatively weaker, possibly because of the losses in the Raman scattered beam while traversing back across A. The width of the peaks is consistent with the focal depth (~95 μm) of the laser beam. The maximum EF observed is ~10^7. This experiment illustrates the feasibility of fabricating cheap, easily deployable, and disposable SERS substrates based on *in situ* generated polymer–metal nanocomposites and a simple and convenient approach to the detection of extremely small amounts of analytes using them.

■ CONCLUSIONS

Polymer–metal nanocomposite thin films formed through a simple *in situ* generation protocol have been used in a wide range of applications earlier. The present study demonstrates the utility of these easily fabricated materials as cheap and convenient SERS substrates for a highly sensitive detection of molecules. A new Ag–polymer nanocomposite thin film is developed by photoirradiation based *in situ* fabrication of the nanoparticles inside the PVVV film. Raman scattering experiments with analyte molecules such as 4-aminothiophenol and Rhodamine 6G indicate that these nanocomposite thin films can routinely produce SERS with EF ~ 10^7. The unique utility of these materials as SERS substrates is demonstrated by fabricating glass capillaries with their inner walls coated with the nanocomposite thin film that can be used to pick up tiny volumes of highly dilute analyte solutions and directly record their Raman spectra. The ease of fabrication and use, coupled with the low cost of the materials and processes involved, make these SERS substrates of considerable value in analytical applications.

dx.doi.org/10.1021/la402594j | *Langmuir* 2013, 29, 13050–13057

■ ASSOCIATED CONTENT

Supporting Information

Details of the calculation of enhancement factor (EF), X-ray diffraction analysis of the reference crystals, EF's for various silver−polymer composite thin films, laser power dependent SERS from 4-ATP, spectroscopy of analytes adsorbed on substrates and microscopy of substrates, determination of the limits of detection. This material is available free of charge via the Internet at http://pubs.acs.org.

■ AUTHOR INFORMATION

Corresponding Author

*E-mail tpr@uohyd.ac.in; Ph 91-40-2313-4827; Fax 91-40-2301-2460 (T.P.R.).

Notes

The authors declare no competing financial interest.

■ ACKNOWLEDGMENTS

Financial support from the Department of Science and Technology, New Delhi, and infrastructure support from the Centre for Nanotechnology and the FESEM facility (School of Physics) at the University of Hyderabad are acknowledged with gratitude. We thank Mr. M. Durga Prasad, Mr. M. Laxminarayana, and Ms. Deepthi for help with the TEM, FESEM, and confocal Raman studies, respectively. E.H. thanks the CSIR, New Delhi, for a senior research fellowship.

■ REFERENCES

(1) Sharma, B.; Frontiera, R. R.; Henry, A.; Ringe, E.; Van Duyne, R. P. SERS: Materials, applications, and the future. *Mater. Today* **2012**, *15*, 16−25.

(2) Graham, D. The next generation of advanced spectroscopy: surface enhanced Raman scattering from metal nanoparticles. *Angew. Chem., Int. Ed.* **2010**, *49*, 9325−9327.

(3) Lombardi, J. R.; Birke, R. L. A unified view of surface-enhanced Raman scattering. *Acc. Chem. Res.* **2009**, *42*, 734−742.

(4) Fan, M.; Andrade, G. F. S.; Brolo, A. G. A review on the fabrication of substrates for surface enhanced Raman spectroscopy and their applications in analytical chemistry. *Anal. Chim. Acta* **2011**, *693*, 7−25.

(5) Jiang, Z. Y.; Jiang, X. X.; Su, S.; Wei, X. P.; Lee, S. T.; He, Y. Silicon-based reproducible and active surface-enhanced Raman scattering substrates for sensitive, specific, and multiplex DNA detection. *Appl. Phys. Lett.* **2012**, *100*, 203104−1−4.

(6) Freeman, R. G.; Grabar, K. C.; Allison, K. J.; Bright, R. M.; Davis, J. A.; Guthrie, A. P.; Hommer, M. B.; Jackson, M. A.; Smith, P. C.; et al. Self-assembled metal colloid monolayers: An approach to SERS substrates. *Science* **1995**, *267*, 1629−1632.

(7) Guo, H.; Jiang, D.; Li, H.; Xu, S.; Xu, W. Highly efficient construction of silver nanosphere dimers on poly(dimethylsiloxane) sheets for surface-enhanced Raman scattering. *J. Phys. Chem. C* **2013**, *117*, 564−570.

(8) Lu, Y.; Liu, G. L.; Lee, L. P. High-density silver nanoparticle film with temperature-controllable interparticle spacing for a tunable surface enhanced Raman scattering substrate. *Nano Lett.* **2005**, *5*, 5−9.

(9) Qian, K.; Liu, H.; Yang, L.; Liu, J. Designing and fabricating of surface-enhanced Raman scattering substrate with high density hot spots by polyaniline template-assisted self-assembly. *Nanoscale* **2012**, *4*, 6449−6454.

(10) Xu, W.; Ling, X.; Xiao, J.; Dresselhaus, M. S.; Kong, J.; Xu, H.; Liu, Z.; Zhang, J. Surface enhanced Raman spectroscopy on a flat graphene surface. *Proc. Natl. Acad. Sci. U. S. A.* **2012**, *109*, 9281−9286.

(11) Cui, Y.; Wang, T.; Zhou, D.; Cheng, Q.; Zhang, C.; Sun, S.; Liu, W.; Han, B. Growth of silver film on graphene oxide pattern. *J. Phys. Chem. C* **2012**, *116*, 17698−17704.

(12) Jian-Wei, L.; Jin-Long, W.; Wei-Ran, H.; Le, Y.; Xi-Feng, R.; Wu-Cheng, W.; Shu-Hong, Y. Ordering Ag nanowire arrays by a glass capillary: A portable, reusable and durable SERS substrate. *Sci. Rep.* **2012**, *2*, 987−1−7.

(13) Schmidt, M. S.; Huebner, J.; Boisen, A. Large area fabrication of leaning silicon nanopillars for surface enhanced Raman spectroscopy. *Adv. Mater.* **2012**, *24*, OP11−OP18.

(14) An, Q.; Zhang, P.; Li, J.; Ma, W.; Guo, J.; Hu, J.; Wang, C. Silver-coated magnetite−carbon core−shell microspheres as substrate-enhanced SERS probes for detection of trace persistent organic pollutants. *Nanoscale* **2012**, *4*, 5210−5216.

(15) Kodiyath, R.; Papadopoulos, T. A.; Wang, J.; Combs, Z. A.; Li, H.; Brown, R. J. C.; Bredas, J.; Tsukruk, V. V. Silver-decorated cylindrical nanopores: Combining the third dimension with chemical enhancement for efficient trace chemical detection with SERS. *J. Phys. Chem. C* **2012**, *116*, 13917−13927.

(16) Cheng, M.; Tsai, B.; Yang, J. Silver nanoparticle-treated filter paper as a highly sensitive surface-enhanced Raman scattering (SERS) substrate for detection of tyrosine in aqueous solution. *Anal. Chim. Acta* **2011**, *708*, 89−96.

(17) Yu, W.; White, I. M. Inkjet printed surface enhanced Raman spectroscopy array on cellulose paper. *Anal. Chem.* **2010**, *82*, 9626−9630.

(18) Gutes, A.; Carraro, C.; Maboudian, R. Silver dendrites from galvanic displacement on commercial aluminum foil as an effective SERS substrate. *J. Am. Chem. Soc.* **2010**, *132*, 1476−1477.

(19) Im, H.; Bantz, K. C.; Lindquist, N. C.; Haynes, C. L.; Oh, S. Vertically oriented sub-10 nm plasmonic nanogap arrays. *Nano Lett.* **2010**, *10*, 2231−2236.

(20) Oh, Y.; Jeong, K. Glass nanopillar arrays with nanogap-rich silver nanoislands for highly intense surface enhanced Raman scattering. *Adv. Mater.* **2012**, *24*, 2234−2237.

(21) Wu, H.; Choi, C. J.; Cunningham, B. T. Plasmonic nanogap-enhanced Raman scattering using a resonant nanodome array. *Small* **2012**, *8*, 2878−2885.

(22) Siddhanta, S.; Thakur, V.; Narayana, C.; Shivaprasad, S. M. Universal metal-semiconductor hybrid nanostructured SERS substrate for biosensing. *ACS Appl. Mater. Interfaces* **2012**, *4*, 5807−5812.

(23) Kahraman, M.; Cakmakyapan, S.; Ozbay, E.; Culha, M. An array of surface-enhanced Raman scattering substrates based on plasmonic lenses. *Ann. Phys.* **2012**, *524*, 663−669.

(24) Yang, L.; Liu, H.; Wang, J.; Zhou, F.; Tian, Z.; Liu, J. Metastable state nanoparticle-enhanced Raman spectroscopy for highly sensitive detection. *Chem. Commun.* **2011**, *47*, 3583−3585.

(25) Yu, D.; Lin, W.; Lin, C.; Chang, L.; Yang, M. An in situ reduction method for preparing silver/poly(vinyl alcohol) nanocomposite as surface-enhanced Raman scattering (SERS)-active substrates. *Mater. Chem. Phys.* **2007**, *101*, 93−98.

(26) Karabicak, S.; Kaya, M.; Vo-Dinh, T.; Volkan, M. *J.* Silver nanoparticle-doped polyvinyl alcohol coating as a medium for surface-enhanced Raman scattering analysis. *Nanosci. Nanotechnol.* **2008**, *8*, 955−960.

(27) He, D.; Hu, B.; Yao, Q.; Wang, K. Yu, Sh. Large-scale synthesis of flexible free-standing SERS substrates with high sensitivity: Electrospun PVA nanofibers embedded with controlled alignment of silver nanoparticles. *ACS Nano* **2009**, *3*, 3993−4002.

(28) Porel, S.; Singh, S.; Harsha, S. S.; Rao, D. N.; Radhakrishnan, T. P. Nanoparticle-embedded polymer: In situ synthesis, free-standing films with highly monodisperse silver nanoparticles and optical limiting. *Chem. Mater.* **2005**, *17*, 9−12.

(29) Ramesh, G. V.; Porel, S.; Radhakrishnan, T. P. Polymer thin films embedded with in situ grown metal nanoparticles. *Chem. Soc. Rev.* **2009**, *38*, 2646−2656.

(30) Porel, S.; Hebalkar, N.; Sreedhar, B.; Radhakrishnan, T. P. Palladium nanowire from precursor nanowire: Crystal-to-crystal transformation via in situ reduction by polymer matrix. *Adv. Funct. Mater.* **2007**, *17*, 2550−2556.

(31) Ramesh, G. V.; Sreedhar, B.; Radhakrishnan, T. P. Real time monitoring of the in situ growth of silver nanoparticles in a polymer

film under ambient conditions. *Phys. Chem. Chem. Phys.* **2009**, *11*, 10059−10063.
(32) Porel, S.; Venkatram, N.; Rao, D. N.; Radhakrishnan, T. P. Optical power limiting in the femtosecond regime by silver nanoparticle−embedded polymer film. *J. Appl. Phys.* **2007**, *102*, 033107−1−6.
(33) Porel, S.; Ramakrishna, D.; Hariprasad, E.; Dutta Gupta, A.; Radhakrishnan, T. P. Polymer thin film with in situ synthesized silver nanoparticles as a potent reusable bactericide. *Curr. Sci.* **2011**, *101*, 927−934.
(34) Hariprasad, E.; Radhakrishnan, T. P. A highly efficient and extensively reusable "dip catalyst" based on a silver-nanoparticle-embedded polymer thin film. *Chem.—Eur. J.* **2010**, *16*, 14378−14384.
(35) Hariprasad, E.; Radhakrishnan, T. P. Palladium nanoparticle-embedded polymer thin film "dip catalyst" for Suzuki−Miyaura reaction. *ACS Catal.* **2012**, *2*, 1179−1186.
(36) Ramesh, G. V.; Radhakrishnan, T. P. A universal sensor for mercury (Hg, Hg^{I}, Hg^{II}) based on silver nanoparticle-embedded polymer thin film. *ACS Appl. Mater. Interfaces* **2011**, *3*, 988−994.
(37) See Supporting Information for details.
(38) Le Ru, E. C.; Blackie, E.; Meyer, M.; Etchegoin, P. G. Surface enhanced Raman scattering enhancement factors: A comprehensive study. *J. Phys. Chem. C* **2007**, *111*, 13794−13803.
(39) Lin, X.-M.; Cui, Y.; Xu, Y.-H.; Ren, B.; Tian, Z.-Q. Surface-enhanced Raman spectroscopy: Substrate-related issues. *Anal. Bioanal. Chem.* **2009**, *394*, 1729−1745.
(40) Huang, Y.; Wu, D.; Zhu, H.; Zhao, L.; Liu, G.; Ren, B.; Tian, Z. Surface-enhanced Raman spectroscopic study of p-aminothiophenol. *Phys. Chem. Chem. Phys.* **2012**, *14*, 8485−8497.
(41) Choi, H.; Shon, H. K.; Yu, H.; Lee, T. G.; Kim, Z. H. b2 peaks in SERS Spectra of 4-aminobenzenethiol: A photochemical artifact or a real chemical enhancement? *J. Phys. Chem. Lett.* **2013**, *4*, 1079−1086.
(42) Osawa, M.; Matsuda, N.; Yoshii, K.; Uchida, I. Charge transfer resonance Raman process in surface-enhanced Raman scattering from p-aminothiophenol adsorbed on silver: Herzberg-Teller contribution. *J. Phys. Chem.* **1994**, *98*, 12702−12707.
(43) El-Safty, S. A.; Ismail, A. A.; Matsunaga, H.; Nanjo, H.; Mizukami, F. Uniformly mesocaged cubic *Fd3m* monoliths as modal carriers for optical chemosensors. *J. Phys. Chem. C* **2008**, *112*, 4825−4835.
(44) Christian, G. D. *Analytical Chemistry*, 6th ed.; John Wiley & Sons Inc.: New York, 2003.